════════ *Semiconductor physics* ════════

Electrical properties of cation-substituted Ag$_7$(Si$_{1−x}$Ge$_x$)S$_5$I single crystals

I.P. Studenyak[1,*], A.I. Pogodin[1], I.A. Shender[1], M.J. Filep[1,2], O.P. Kokhan[1], P. Kopčanský[3]

[1]Uzhhorod National University, 46, Pidhirna str., 88000 Uzhhorod, Ukraine
[2]Ferenc Rákóczi II Transcarpathian Hungarian Institute, Kossuth Sq. 6, Beregovo 90200, Ukraine
[3]Institute of Experimental Physics, Slovak Academy of Sciences,
47, Watsonova Str., 04001 Košice, Slovakia
**Corresponding author e-mai*l: *studenyak@dr.com*

Abstract. High-quality single crystals of Ag$_7$(Si$_{1−x}$Ge$_x$)S$_5$I (x = 0.2, 0.4, 0.6, 0.8) solid solutions are grown from the solution–melt by vertical zone crystallization method. The measurements of electrical conductivity of Ag$_7$(Si$_{1−x}$Ge$_x$)S$_5$I solid solutions were performed using the impedance spectroscopy method within the frequency range from 10 Hz up to $2 \cdot 10^6$ Hz and temperature interval 293–383 K. Ionic and electronic components of electrical conductivity, as well as their ratios, were determined using the Nyquist plots.

Keywords: argyrodites, crystal structure, superionic conductors, cationic substitution, electrical conductivity.

1. Introduction

Presently, Li$^+$-ion batteries are the most commercially available and distributed secondary energy sources. This spread is caused by a number of advantages, including easy and fast charging, easy maintenance, relatively low self-discharge and high energy density, *etc*. At the same time, it is worth noting that there are certain shortcomings that reduce the efficiency of Li$^+$-ion batteries and bring them closer to their limit of use [1–6]. One of the ways for development is the rejection of flammable liquid electrolyte and the use of an all-solid-state battery [1–3]. This stimulates the search for new materials with high ionic conductivity, which can be used as solid electrolytes.

Among inorganic materials (oxides, phosphates, complex sulfides) that meet the requirements for solid-state ionic conductors sulfur-containing phases are being actively investigated [1, 2, 7]. A large class of ternary and quaternary compounds with a similar crystal structure, united under the name argyrodites [8, 9], is promising in this respect. The most common and studied are argyrodites based on four and five valence elements with the general formula $M_7^+ E^{5+} S_6^{2-}$, $M_6^+ E^{5+} S_5^{2-}$ Hal, $M_8^+ E^{4+} S_6^{2-}$ and $M_7^+ E^{4+} S_5^{2-}$ Hal$^-$ (Me$^+$ = Cu$^+$, Ag$^+$, Li$^+$; E^{5+} = P^{5+}, As^{5+}; E^{4+} = Si^{4+}, Ge^{4+}, Sn^{+4}; Hal$^-$ = Cl$^-$, Br$^-$, I$^-$). These phases show superionic, ferroelastic and thermoelectric properties [10–15], which are caused by the peculiarities of the crystalline structure (the combination of rigid anionic and disordered cationic sublattice) [9]. In recent years, they have been prepared in the forms of composites, ceramics and films [16–19].

The proximity of the crystal lattice parameters [14] determines a significant amount of solid solutions between compounds with the structure of argyrodite formed by both isovalent and heterovalent substitution [20–26]. This is used to optimize the functional parameters of the materials under study.

Ag$_7$SiS$_5$I and Ag$_7$Ges$_5$I compounds crystallize in a face-centred cubic cell ($F\bar{4}3m$) with the lattice parameters: 10.6543 Å and 10.7116 Å, respectively [10]. Ag$_7$SiS$_5$I and Ag$_7$Ges$_5$I are characterized by significant electrical conductivity. Thus, the total electrical conductivity of polycrystalline samples of Ag$_7$SiS$_5$I and Ag$_7$GeS$_5$I is $0.96 \cdot 10^{-2}$ S/cm and $2.77 \cdot 10^{-2}$ S/cm, respectively [10]. In the case of monocrystalline samples, for Ag$_7$SiS$_5$I the total electrical conductivity values are $3.5 \cdot 10^{-2}$ S/cm for Ag$_7$SiS$_5$I [27] and $4.7 \cdot 10^{-2}$ S/cm for Ag$_7$GeS$_5$I [28], while the values of ionic component of electrical conductivity are $8.13 \cdot 10^{-3}$ S/cm [27] and $7.98 \cdot 10^{-3}$ S/cm [28], respectively.

This paper is devoted to the investigation of electrical conductivity of monocrystalline samples of Ag$_7$SiS$_5$I and Ag$_7$GeS$_5$I as well as Ag$_7$(Si$_{1−x}$Ge$_x$)S$_5$I solid solutions on their basis. It is also devoted to determining the values of the ionic and electronic components of electrical conductivity, their activation energies and the influence of isovalent substitution Si^{4+} ↔ Ge^{4+} on the electrical properties of the solid solutions under investigation.

2. Experimental

Synthesis of Ag_7SiS_5I and Ag_7GeS_5I was carried out from simple substances: silver (99.995%), silicon (99.99%), sulfur (99.999%), germanium (99.99%) and presynthesized binary silver (I) iodide, additionally purified using the directional crystallization method, taken in stoichiometric ratios in evacuated up to 0.13 Pa silica ampoules. The synthesis regime for Ag_7SiS_5I and Ag_7GeS_5I included step heating up to 723 K at the rate ≈100 K/h (ageing during 48 hours), further increase of the temperature up to 1273 K at the rate close to 50 K/h and ageing at this temperature for 24 hours. Cooling was performed in the oven off mode.

Alloys of Ag_7SiS_5I-Ag_7GeS_5I system were synthesized using the direct one-temperature method from pre-synthesized quaternary Ag_7SiS_5I and Ag_7GeS_5I. Synthesis mode included stepped heating at the rate close to 100 K/h up to 1273 K and exposure for 72 hours. The annealing temperature was 873 K (120 hours ageing). Cooling to room temperature was carried out in the mode of the switched off oven.

To ascertain the optimal technological regimes for growing single crystals, alloys of solid solutions were investigated using the method of differential thermal analysis (Pt-PtRh thermocouple, heating/cooling rate 700 K/h, accuracy ±2 K). According to the results of differential thermal analysis, it was found that melting temperatures of $Ag_7(Si_{1-x}Ge_x)S_5I$ ($x = 0, 0.2, 0.4, 0.6, 0.8, 1$) were within the temperature range 1166 up to 1172 K. This led to the choice of the same temperature regimes for growing single crystals in the entire concentration interval.

Growing the single crystals of $Ag_7(Si_{1-x}Ge_x)S_5I$ ($x = 0.2, 0.4, 0.6, 0.8$) solid solutions was carried out using the method of vertical zone crystallization from a solution-melt in a two-zone tubular resistance furnace using silica container of special configuration. To homogenize the melt of $Ag_7(Si_{1-x}Ge_x)S_5I$ ($x = 0.2, 0.4, 0.6, 0.8$) solid solutions, 24-hour ampoule ageing at a temperature of 1223 K (~ 50 K more than T_m) in the melt zone was conducted. Growing the single crystal consists of formation of the seed in the lower conical part of the container using the method of recrystallization in the course of 24 hours and the crystal build-up on the formed seed. The optimum velocity of crystallization front movement was 0.4–0.5 mm/h, the annealing temperature was determined to be 873 K (72 hour), cooling rate to room temperature was 5 K/h. By using this method, $Ag_7(Si_{1-x}Ge_x)S_5I$ solid solutions, characterized by dark grey colour and a metallic luster, 30–40 mm in length and 10–12 mm in diameter were obtained.

Investigations of electrical conductivity of $Ag_7(Si_{1-x}Ge_x)S_5I$ ($x = 0.2, 0.4, 0.6, 0.8$) solid solutions were carried out using impedance spectroscopy [29] in the frequency range from 10 Hz up to $2 \cdot 10^6$ Hz and temperature interval 293–383 K ranges using high-precision LCR meters Keysight E4980A and AT 2818. The amplitude of the alternating current constituted 10 mV. Measurements were carried out using the two-electrode method with blocking gold contacts that were applied by chemical precipitation from solutions [27]. The analysis of the received dependences, using the Nyquist plots, was carried out in the program ZView 3.5.

3. Results and discussion

Fig. 1 shows the frequency dependences of the total electrical conductivity for $Ag_7(Si_{1-x}Ge_x)S_5I$ solid solutions. For all the compositions, the frequency dependences of the total electrical conductivity show the increase of the conductivity with increasing frequency, which is typical for materials with ionic conductivity in solid state. The character of the frequency dependences for all solid solutions indicates their belonging to ionic-electronic conductors, for which $\sigma_{ion} \gg \sigma_{el}$.

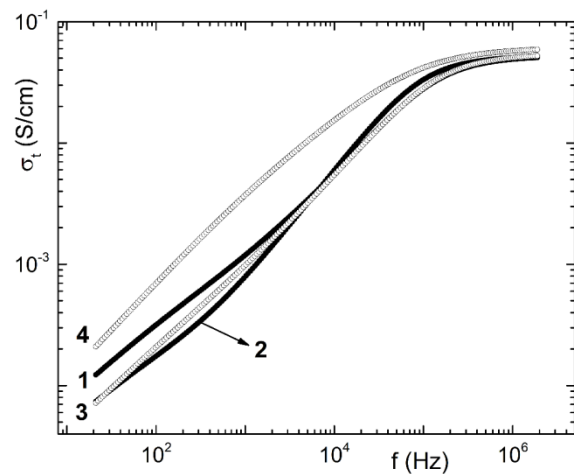**Fig. 1.** Frequency dependences of total electrical conductivity at $T = 298$ K for $Ag_7(Si_{1-x}Ge_x)S_5I$ solid solutions: (*1*) $Ag_7(Si_{0.8}Ge_{0.2})S_5I$, (*2*) $Ag_7(Si_{0.6}Ge_{0.4})S_5I$, (*3*) $Ag_7(Si_{0.4}Ge_{0.6})S_5I$, and (*4*) $Ag_7(Si_{0.2}Ge_{0.8})S_5I$.

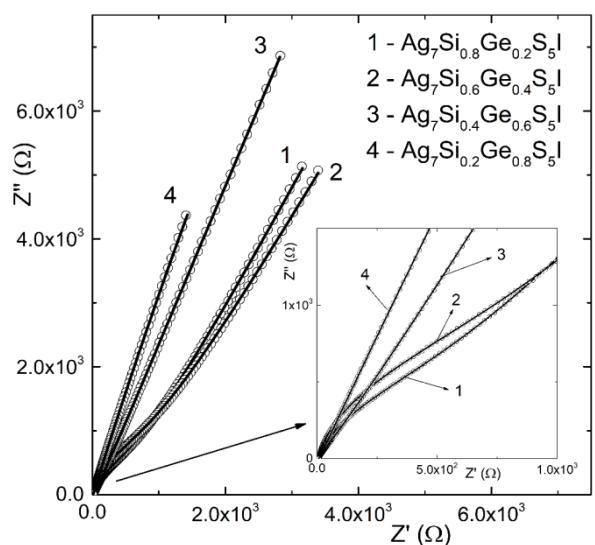**Fig. 2.** Nyquist plots at $T = 298$ K for $Ag_7(Si_{1-x}Ge_x)S_5I$ solid solutions: experimental data correspond to the solid lines, calculated data correspond to the open dots.

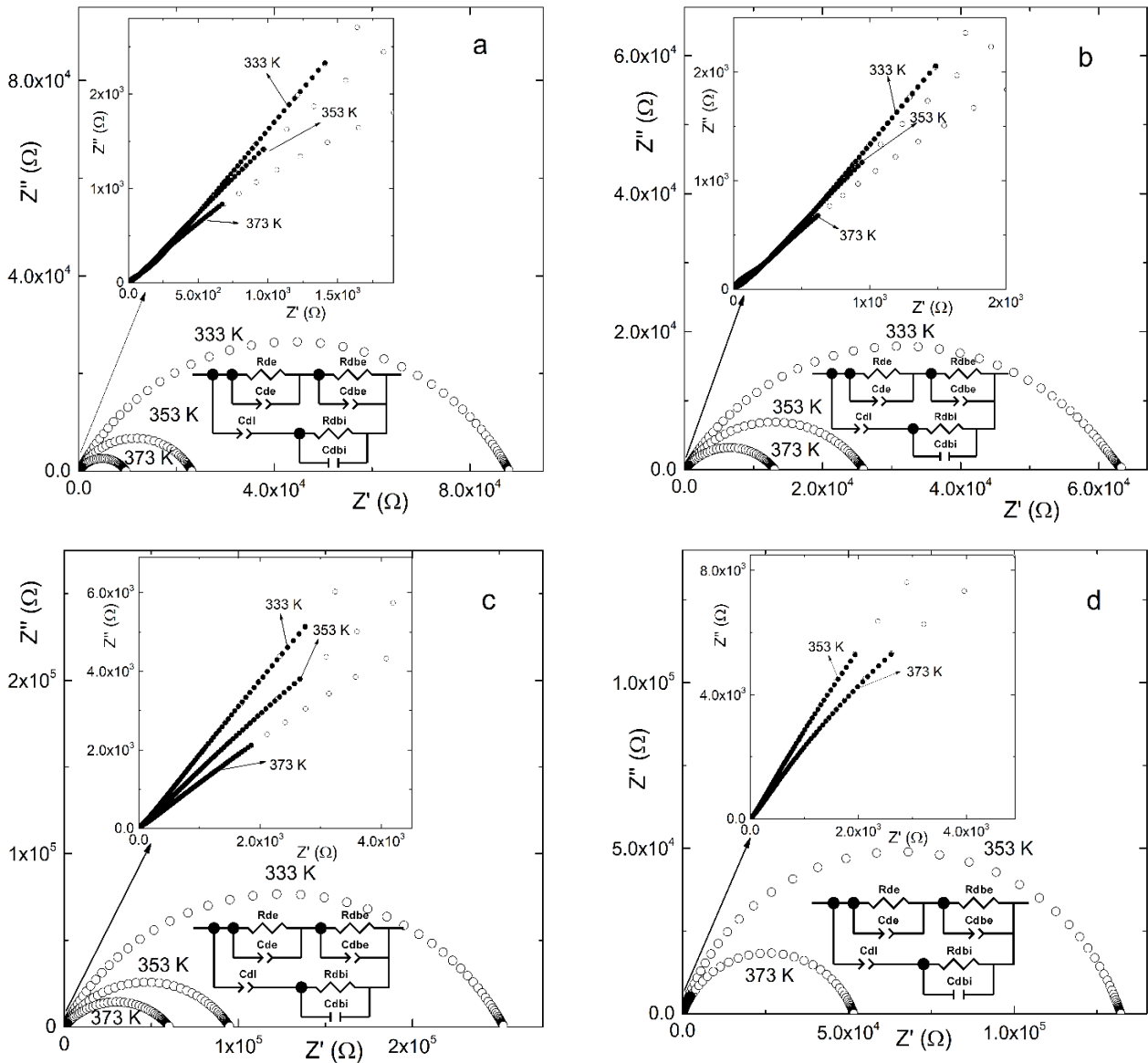*Studenyak I.P., Pogodin A.I., Shender I.A. et al. Electrical properties of cation-substituted Ag₇(Si₁₋ₓGeₓ)S₅I ...*

242

Fig. 3. EEC and Nyquist plots for $Ag_7(Si_{1-x}Ge_x)S_5I$ solid solutions at different temperatures: (a) $Ag_7(Si_{0.8}Ge_{0.2})S_5I$, (b) $Ag_7(Si_{0.6}Ge_{0.4})S_5I$, (c) $Ag_7(Si_{0.4}Ge_{0.6})S_5I$, and (d) $Ag_7(Si_{0.2}Ge_{0.8})S_5I$. Experimental data correspond to the solid dots, calculated data correspond to the open dots.

The standard approach based on electrode equivalent circuits (EEC) [29–31] and their analysis on Nyquist plots were used for detailed studies of the frequency dependences of electrical conductivity and its separation into ionic and electronic components. The parasitic inductance of the cell ($\sim 2 \cdot 10^{-8}$ H) was taken into account during the performed analysis.

The monocrystalline samples of $Ag_7(Si_{1-x}Ge_x)S_5I$ ($x = 0.2$, 0.4, 0.6, 0.8) solid solutions are characterized by a rather low electronic ($\sigma_{ion} \gg \sigma_{el}$) and high values of ionic conductivity components, which led to the shift of the low-frequency semicircle to the low-frequency region, which is the evidence of the influence of diffusion and relaxation processes.

This feature significantly influenced the character of the frequency dependences of total electrical conductivity

for $Ag_7(Si_{1-x}Ge_x)S_5I$ solid solutions (Fig. 1) and caused some difficulties in the process of their analysis on Nyquist plots using EEC. This is primarily due to the limited 10 Hz frequency range. As a result, for $Ag_7(Si_{1-x}Ge_x)S_5I$ solid solutions it was impossible to determine the electronic component of electrical conductivity with sufficient accuracy in the following temperature intervals: for $x = 0.2$, 0.4 within the interval 293–323 K, for $x = 0.6$ within the interval 293–303 K, and for $x = 0.8$ within the interval 293–343 K.

Also unsuccessful was the attempt to solve this problem by changing the geometric dimensions of the samples (increasing the ratio of area to thickness), which is probably associated with significant values of activation energy of the electronic component of electrical conductivity.
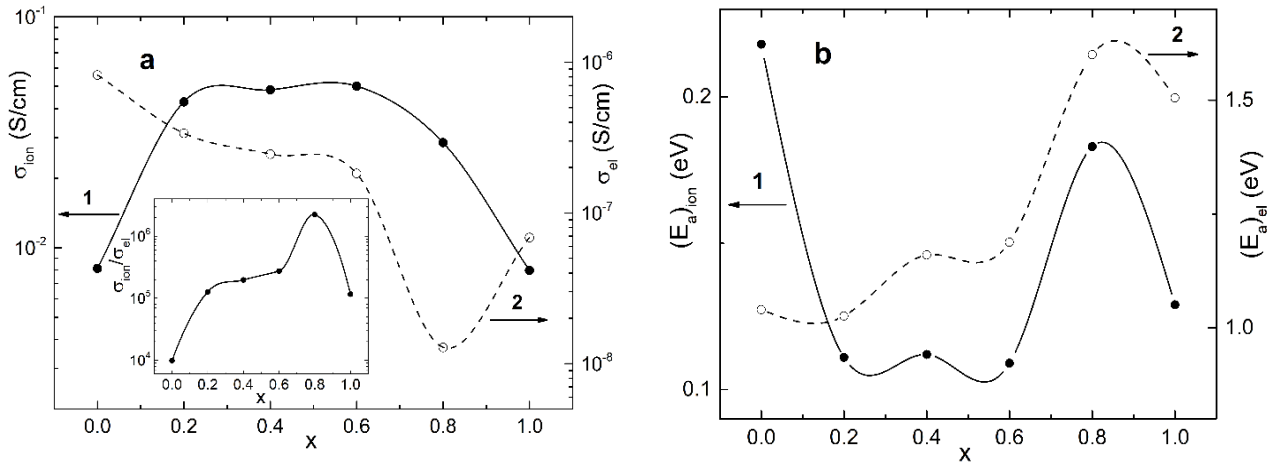
Studenyak I.P., Pogodin A.I., Shender I.A. et al. Electrical properties of cation-substituted $Ag_7(Si_{1-x}Ge_x)S_5I$ ...

243

Fig. 4. Compositional dependences of ionic (*1*) and electronic (*2*) components of electrical conductivity (a) and activation energies of ionic (*1*) and electronic (*2*) components of electrical conductivity (b) at $T = 298$ K for $Ag_7(Si_{1-x}Ge_x)S_5I$ solid solutions. The insert shows the compositional dependence of the ratio of the ionic component of electrical conductivity to the electronic one for $Ag_7(Si_{1-x}Ge_x)S_5I$ solid solutions.

On Z'-Z" dependences, two semicircles were observed for all solid solutions, but it remains noteworthy that the high-frequency semicircle for $Ag_7(Si_{0.4}Ge_{0.6})S_5I$ and $Ag_7(Si_{0.2}Ge_{0.8})S_5I$ solid solutions is very weakly expressed throughout the temperature range under study (Fig. 2, curves *3* and *4*; Fig. 3, curves *c* and *d*). In respect to the above features, for $T = 298$ K (Fig. 2), only a high-frequency semicircle and a low-frequency section (a component of the corresponding semicircle) described with EEC (Fig. 3) are presented.

To describe the Nyquist plots for all solid solutions, one EEC was selected (Fig. 3), which can be separated into two parts: ionic, which includes a description of the processes associated with the ionic component of conductivity, and electronic one, which is responsible for the electronic component of electrical conductivity, respectively.

Low-frequency semicircles/areas in the Nyquist plots correspond to the diffusion relaxation processes on the electrode/crystal boundary, which is expressed *via* the included capacitance of the double diffusion layer C_{dl} (Fig. 3). The prevailing influence of diffusion and ionic relaxation processes, against the background of sufficiently low specific value of electronic and high values of ionic components of electrical conductivity, lead to a fuzzy representation of high-frequency semicircles, which in turn are described by the processes of electrical conductivity on domain boundaries for which the connected resistance R_{dbi} (Fig. 3) with a parallel capacitance C_{dbi} corresponds in EEC. Thus, the ionic conductivity of $Ag_7(Si_{1-x}Ge_x)S_5I$ ($x = 0.2, 0.4, 0.6, 0.8$) solid solutions is defined by the resistance of domain boundaries R_{dbi}.

Parallelly to the parameters responsible for the ionic component of electrical conductivity in EEC, the parameters responsible for the electronic component of electrical conductivity are included, namely: the electronic resistance of domains R_{de} and the electronic

resistance of the domain boundaries R_{dbe} with parallel capacitances C_{de} and C_{dbe}, respectively, which contributes to the representation of both semicircles in the Nyquist plots. Consequently, the electronic component of electrical conductivity of $Ag_7(Si_{1-x}Ge_x)S_5I$ ($x = 0.2, 0.4, 0.6, 0.8$) solid solutions is defined by the sum of the resistance of domain boundaries R_{dbe} and the resistance of domains R_{de}.

EEC shown in Fig. 3 describes the temperature behaviour of impedance inherent to these solid solutions in the entire temperature range under study (Figs 2 and 3) and is well consistent with the description of all ionic and electronic processes. During the temperature increase, a sequential degeneration of two semicircles into one is observed, which is especially noticeable for $Ag_7(Si_{0.8}Ge_{0.2})S_5I$ and $Ag_7(Si_{0.6}Ge_{0.4})S_5I$ solid solutions at the temperature close to 373 K (Figs 3c and 3d) due to a significant increase in the ionic component of electrical conductivity.

The analysis of impedance spectra made it possible to investigate compositional (Fig. 4a) and temperature (Fig. 5) dependences of ionic and electronic components of electrical conductivity for $Ag_7(Si_{1-x}Ge_x)S_5I$ ($x = 0.2, 0.4, 0.6, 0.8$) solid solutions. It was ascertained that iso-valent cationic $Si^{+4} \rightarrow Ge^{+4}$ substitution leads to a nonli-near compositional dependence of the ionic component of electrical conductivity (Fig. 4a, curve *1*), which mani-fests itself in its sharp increase, as compared to the initial quaternary Ag_7SiS_5I and Ag_7GeS_5I. Thus, if the value of the ionic component of electrical conductivity constitutes of $8.13 \cdot 10^{-3}$ S/cm [27] for Ag_7SiS_5I and $7.98 \cdot 10^{-3}$ S/cm [28] for Ag_7GeS_5I, then for $Ag_7(Si_{1-x}Ge_x)S_5I$ solid solutions its value lies within the range from $2.85 \cdot 10^{-2}$ to $5.00 \cdot 10^{-2}$ S/cm. The values of the electronic component of electrical conductivity (Fig. 4a, curve *2*) were deter-mined by extrapolation of linear sections of temperature dependences (Fig. 5, lines *2*). Thus, the compositional dependence (Fig. 4a, curve *2*) for $Ag_7(Si_{0.2}Ge_{0.8})S_5I$

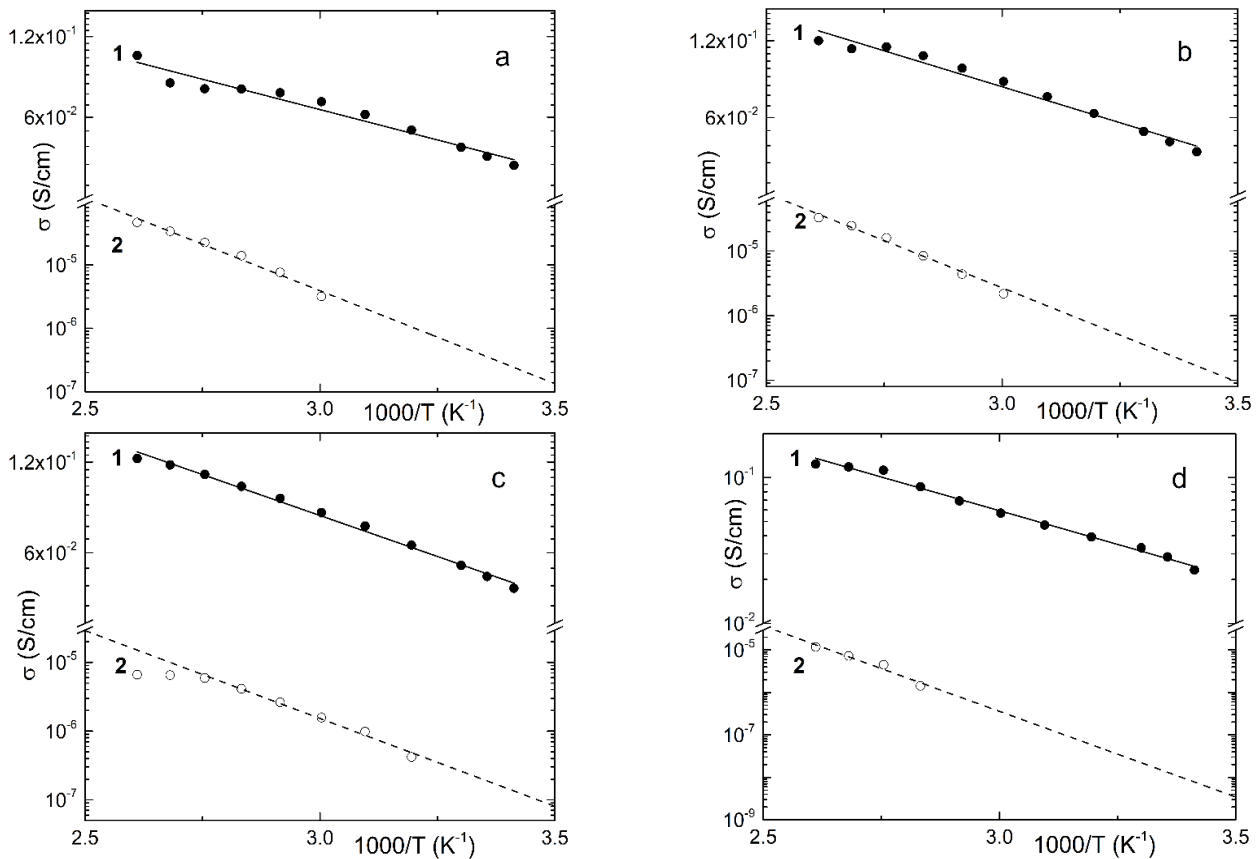*Studenyak I.P., Pogodin A.I., Shender I.A. et al. Electrical properties of cation-substituted Ag₇(Si₁₋ₓGeₓ)S₅I …*

244

Fig. 5. Temperature dependences of ionic (*1*) and electronic (*2*) components inherent to the electrical conductivity of $Ag_7(Si_{1-x}Ge_x)S_5I$ solid solutions: (a) $Ag_7(Si_{0.8}Ge_{0.2})S_5I$, (b) $Ag_7(Si_{0.6}Ge_{0.4})S_5I$, (c) $Ag_7(Si_{0.4}Ge_{0.6})S_5I$, and (d) $Ag_7(Si_{0.2}Ge_{0.8})S_5I$.

solid solution shows a minimum of the electronic component of conductivity ($\sim 1.3 \cdot 10^{-8}$ S/cm).

In the insert to Fig. 4a, the compositional dependence of the ratio of ionic component of electrical conductivity to the electronic one is shown. As a result, it was ascertained that for $Ag_7(Si_{1-x}Ge_x)S_5I$ (x = 0.2, 0.4, 0.6) solid solutions, the ionic component is more than 10^5 times higher than the electronic one and for $Ag_7(Si_{0.2}Ge_{0.8})S_5I$ solid solution, the ratio σ_{ion}/σ_{el} is 10^6.

In Fig. 5, the temperature dependences of the ionic (lines *1*) and electronic (lines *2*) components of electrical conductivity in Arrhenius coordinates are shown. It is ascertained that they are linear and are described by the Arrhenius law, which testifies to the thermoactivating character of conductivity. With their help, the activation energy was determined both for the ionic and for the electronic components of electrical conductivity (Fig. 4b). On the compositional dependence of the activation energy of ionic conductivity (Fig. 4b, curve *1*), a nonlinear decrease in the activation energy for $Ag_7(Si_{1-x}Ge_x)S_5I$ (x = 0.2, 0.4, 0.6) solid solutions, and its maximum for $Ag_7(Si_{0.2}Ge_{0.8})S_5I$ were found. In this case, the activation energy of the electronic component of electrical conductivity after cationic $Si^{+4} \rightarrow Ge^{+4}$ substitution (Fig. 4b, curve *2*) increases nonlinearly, and is characterized by the presence of a maximum for a solid solution of similar composition ($Ag_7(Si_{0.2}Ge_{0.8})S_5I$).

4. Conclusions

Synthesis of $Ag_7(Si_{1-x}Ge_x)S_5I$ (x = 0.2, 0.4, 0.6, 0.8) solid solutions was carried out, and using vertical zone crystallization method the single crystals of dark grey colour with metallic luster were grown from solution-melt with the length 30–40 mm and diameter 10–12 mm.

Total electrical conductivity was measured using impedance spectroscopy with gold contacts in the frequency range from 10 Hz up to $2 \cdot 10^6$ Hz and temperature range 293–383 K in monocrystalline samples of $Ag_7(Si_{1-x}Ge_x)S_5I$ (x = 0.2, 0.4, 0.6, 0.8) solid solutions. Being based on the frequency dependences of the total electrical conductivity, the Nyquist plots were plotted and then analyzed using electrode equivalent circuits. Using this approach, the total electrical conductivity was separated into ionic and electronic components, which allowed plotting their compositional dependence and to determine the σ_{ion}/σ_{el} ratio. It has been ascertained that the temperature dependences of the ionic and electronic components of electrical conductivity are linear and described by the Arrhenius law, which indicates the thermoactivation mechanism of conductivity. According to the results of temperature studies, activation energies of both ionic and electronic component of electrical conductivity have been determined.

Studenyak I.P., Pogodin A.I., Shender I.A. et al. Electrical properties of cation-substituted Ag₇(Si₁₋ₓGeₓ)S₅I ...

245

References

1. Kim T., Song W., Son D.-Y., Ono L.K., Qi Y. Lithium-ionbatteries: outlook on present, future, and hybridized technologies. *J. Mater. Chem. A.* 2019. **7**. P. 2942–2964. https://doi.org/10.1039/c8ta10513h.

2. Miao Y., Hynan P., Jouannevon A., Yokochi A. Current Li-ion battery technologies in electric vehicles and opportunities for advancements. *Energies.* 2019. **12**. P. 1074. https://doi.org/10.3390/en12061074.

3. Ohno S., Banik A., Dewald G.F. *et al.* Materials design of ionic conductors for solid state batteries. *Prog. Energy.* 2020. **2**. P. 022001. https://doi.org/10.1088/2516-1083/ab73dd.

4. Grey C.P., Hall D.S. Prospects for lithium-ion batteries and beyond – a 2030 vision. *Nat. Commun.* 2020. **11**. P. 6279. https://doi.org/10.1038/s41467-020-19991-4.

5. Duan J., Tang X., Dai H. *et al.* Building safe lithium-ion batteries for electric vehicles: a review. *Electrochem. Energ. Rev.* 2020. **3**. P. 1–42. https://doi.org/10.1007/s41918-019-00060-4.

6. Chen Y., Wen K., Chen T. *et al.* Recent progress in all-solid-state lithium batteries: The emerging strategies for advanced electrolytes and their interfaces. *Energy Storage Mater.* 2020. **31**. P. 401–433. https://doi.org/10.1016/j.ensm.2020.05.019.

7. Reddy M.V., Julien C.M., Mauger A., Zaghib K. Sulfide and oxide inorganic solid electrolytes for all-solid-state Li batteries: A review. *Nanomaterials.* 2020. **10**. P. 1606. https://doi.org/10.3390/nano10081606.

8. Kuhs W.F., Nitsche R., Scheunemann K. The argyrodites – a new family of tetrahedrally close-packed structures. *Mat. Res. Bull.* 1979. **14**. P. 241–248. https://doi.org/10.1016/0025-5408(79)90125-9.

9. Nilges T., Pfitzner A. A structural differentiation of quaternary copper argyrodites: Structure – property relations of high temperature ion conductors. *Z. Kristallogr.* 2005. **220**. P. 281–294. https://doi.org/10.1524/zkri.220.2.281.59142.

10. Laqibi M., Cros B., Peytavin S., Ribes M. New silver superionic conductors Ag_7XY_5Z (X = Si, Ge, Sn; Y = S, Se; Z = Cl, Br, I)-synthesis and electrical studies. *Solid State Ionics.* 1987. **23**, No 1–2. P. 21–26. https://doi.org/10.1016/0167-2738(87)90077-4.

11. Deiseroth H.-J., Maier J., Weichert K. *et al.* Li_7PS_6 and Li_6PS_5X (X: Cl, Br, I): possible three-dimensional diffusion pathways for lithium ions and temperature dependence of the ionic conductivity

by impedance measurements. *Z. Anorg. Allg. Chem.* 2011. **637**. P. 1287–1294. https://doi.org/10.1002/zaac.201100158.

12. Haznar A., Pietraszko A., Studenyak I.P. X-ray study of the superionic phase transition in Cu_6PS_5Br. *Solid State Ionics.* 1999. **119**, No 1–4. P. 31–36. https://doi.org/10.1016/S0167-2738(98)00479-2.

13. Fan Y., Wang G., Wang R. *et al.* Enhanced thermoelectric properties of *p*-type argyrodites Cu_8GeS_6 through Cu vacancy. *J. Alloys and Compd.* 2020. **822**. P. 153665. https://doi.org/10.1016/j.jallcom.2020.153665.

14. Beeken R.B., Garbe J.J., Gillis J.M. *et al.* Electrical conductivities of the Ag_6PS_5X and the Cu_6PSe_5X (X = Br, I) argyrodites. *J. Phys. Chem. Solids.* 2005. **66**, No 5. P. 882–886. https://doi.org/10.1016/j.jpcs.2004.10.010.

15. Studenyak I.P., Kranjcec M., Bilanchuk V.V. *et al.* Temperature variation of electrical conductivity and absorption edge in Cu_7GeSe_5I advanced superionic conductor. *J. Phys. Chem. Solids.* 2009. **70**. P. 1478–1481. https://doi.org/10.1016/j.jpcs.2009.09.003.

16. Orliukas A.F., Kazakevicius E., Kezionis A. *et al.* Preparation, electric conductivity and dielectrical properties of Cu_6PS_5I-based superionic composites. *Solid State Ionics.* 2009. **180**, No 2–3. P. 183–186. https://doi.org/10.1016/j.ssi.2008.12.005.

17. Studenyak I.P., Izai V.Yu., Studenyak V.I. *et al.* Influence of Cu_6PS_5I superionic nanoparticles on the dielectric properties of 6CB liquid crystal. *Liquid Crystals.* 2017. **44**, No 5. P. 897–903. https://doi.org/10.1080/02678292.2016.1254288.

18. Šalkus T., Kazakevičius E., Banys J. *et al.* Influence of grain size effect on electrical properties of Cu_6PS_5I superionic ceramics. *Solid State Ionics.* 2014. **262**. P. 597–600. https://doi.org/10.1016/j.ssi.2013.10.040.

19. Studenyak I.P., Kranjčec M., Izai V.Yu. *et al.* Structural and temperature-related disordering studies of Cu_6PS_5I amorphous thin films. *Thin Solid Films.* 2012. **520**, No 6. P. 1729–1733. https://doi.org/10.1016/j.tsf.2011.08.043.

20. Studenyak I.P., Kranjčec M., Kovacs Gy.S. *et al.* The excitonic processes and Urbach rule in $Cu_6P(S_{1-x}Se_x)_5I$ crystals in the sulfur-rich region. *Mat. Res. Bull.* 2001. **36**, No 1–2. P. 123–135. https://doi.org/10.1016/S0025-5408(01)00508-6.

21. Kranjčec M., Studenyak I.P., Kurik M.V. Urbach rule and disordering processes in $Cu_6P(S_{1-x}Se_x)_5Br_{1-y}I_y$ superionic conductors. *J. Phys. Chem. Solids.* 2006. **67**, No 4. P. 807–817. https://doi.org/10.1016/j.jpcs.2005.10.184.

22. Kraft M.A., Ohno S., Zinkevich T. *et al.* Inducing high ionic conductivity in the lithium superionic argyrodites $Li_{6+x}P_{1-x}Ge_xS_5I$ for all-solid-state batteries. *J. Am. Chem. Soc.* 2018. **140**. P. 16330–16339. https://doi.org/10.1021/jacs.8b10282.

23. Pogodin A.I., Filep M.J., Malakhovska T.O. *et al.* The copper argyrodites $Cu_{7-n}PS_{6-n}Br_n$: Crystal growth, structures and ionic conductivity. *Solid State Ionics.* 2019. **341**. 115023. https://doi.org/10.1016/j.ssi.2019.115023.

Studenyak I.P., Pogodin A.I., Shender I.A. et al. Electrical properties of cation-substituted Ag$_7$(Si$_{1-x}$Ge$_x$)S$_5$I …

246

24. Adeli P., Bazak J.D., Park K.H. *et al.* Boosting solid state diffusivity and conductivity in lithium superionic argyrodites by halide substitution. *Angew. Chem. Int. Ed.* 2019. **58**. P. 8681–8686. https://doi.org/10.1002/anie.201814222.

25. Studenyak I.P., Izai V.Yu., Studenyak V.I. *et al.* Interrelations between structural and optical properties of $(Cu_{1-x}Ag_x)_7GeS_5I$ mixed crystals. *Ukr. J. Phys. Opt.* 2018. **19**. P. 237–243. https://doi.org/10.3116/16091833/19/4/237/2018.

26. Minafra N., Culver S.P., Krauskopf T., Senyshyn A., Zeier W.G. Effect of Si substitution on the structural and transport properties of superionic Li-argyrodites. *J. Mater. Chem. A*. 2018. **6**. P. 645–651. https://doi.org/10.1039/C7TA08581H.

27. Studenyak I.P., Pogodin A.I., Studenyak V.I. *et al.* Electrical properties of copper- and silver-containing superionic $(Cu_{1-x}Ag_x)_7SiS_5I$ mixed crystals with argyrodite structure. *Solid State Ionics*. 2020. **345**. P. 115183. https://doi.org/10.1016/j.ssi.2019.115183.

28. Studenyak I.P., Pogodin A.I., Studenyak V.I. *et al.* Structure, electrical conductivity, and Raman spectra of $(Cu_{1-x}Ag_x)_7GeS_5I$ and $(Cu_{1-x}Ag_x)_7GeSe_5I$ mixed crystals. *Mater. Res. Bull.* 2021. **135**. P. 111116. https://doi.org/10.1016/j.materresbull.2020.111116.

29. Orazem M.E., Tribollet B. *Electrochemical Impedance Spectroscopy*. New Jersey: John Wiley & Sons, 2008. https://doi.org/10.1002/9780470381588.

30. Ivanov-Schitz A.K., Murin I.V. *Solid State Ionics*. St.-Petersburg: Univ. Press, 2000 (in Russian).

31. Huggins R.A. Simple method to determine electronic and ionic components of the conductivity in mixed conductors a review. *Ionics*. 2002. **8**, No 3. P. 300–313. https://doi.org/10.1007/BF02376083.

Authors and CV

Artem I. Pogodin, defended his PhD thesis in inorganic chemistry in 2016. Senior researcher at the Uzhhorod National University. Authored over 35 articles and 25 patents. The area of his scientific interests includes solid state chemistry, crystal growth, and materials science. https://orcid.org/0000-0002-2430-3220; artempogodin88@gmail.com

Iryna A. Shender, born in 1995. Currently she is PhD student at the Uzhhorod National University, Faculty of Physics. The area of scientific interests is electrical and optical properties of superionic conductors. https://orcid.org/0000-0003-1687-3634 shender95@gmail.com

Mykhailo J. Filep, born in 1987, defended his PhD thesis in inorganic chemistry in 2015. Senior researcher at the Uzhhorod National University. Authored over 40 articles and 20 patents. The area of his scientific interests includes solid state chemistry and materials science. mfilep23@gmail.com http://orcid.org/0000-0001-7017-5437

Oleksandr P. Kokhan, PhD, Associate professor of Inorganic Chemistry department, Uzhhorod National University. Authored over 80 articles and 40 patents. The area of his interests includes inorganic chemistry, solid state chemistry, crystal growth, materials science. aleksandr.kokh@gmail.com, http://orcid.org/0000-0003-1534-6779

Ihor P. Studenyak, Dr. Sc. in Physics and Mathematics. Vice-rector for research at the Uzhhorod National University. Authored over 200 publications, 120 patents, 15 text-books. The area of his scientific interests includes physical properties of semiconductors, ferroics and superionic conductors. https://orcid.org/0000-0001-9871-5773

Peter Kopčanský, Professor, Senior researcher of Institute of Experimental Physics, Slovak Academy of Sciences. Authored over 250 articles, 6 patents, 1 monograph, 5 textbooks. The area of his scientific interests includes solid state physics, magnetism, transport properties in disordered systems, magnetic fluids, their magnetic and dielectric properties, composite systems with liquid crystals. kopcan@saske.sk, https://orcid.org/0000-0002-5278-9504

Електричні властивості заміщених катіоном монокристалів $Ag_7(Si_{1-x}Ge_x)S_5I$

І.П. Студеняк, А.І. Погодін, І.А. Шендер, М.Й. Філеп, О.П. Кохан, Р. Копčанський

Анотація. Якісні монокристали твердих розчинів $Ag_7(Si_{1-x}Ge_x)S_5I$ (x = 0.2, 0.4, 0.6, 0.8) вирощені із розчину-розплаву методом вертикальної зонної кристалізації. Вимірювання електропровідності твердих розчинів $Ag_7(Si_{1-x}Ge_x)S_5I$ проведено методом імпедансної спектроскопії в діапазоні частот від 10 Гц до $2 \cdot 10^6$ Гц та температурному інтервалі 293–383 K. Іонні та електронні компоненти електропровідності, а також їх співвідношення визначали за допомогою діаграм Найквіста.

Ключові слова: аргіродіти, кристалічна структура, суперіонні провідники, катіонне заміщення, електропровідність.

Studenyak I.P., Pogodin A.I., Shender I.A. et al. Electrical properties of cation-substituted $Ag_7(Si_{1-x}Ge_x)S_5I$ ...

247